Turkish Journal of Chemistry

http://journals.tubitak.gov.tr/chem/

Research Article

Turk J Chem
(2015) 39: 64 – 83

doi:10.3906/kim-1401-91

Synthesis and molecular modeling studies of naproxen-based acyl hydrazone derivatives

Tuğba TAŞKIN TOK[1,*], Özgün ÖZAŞIK[2], Deniz SARIGÖL[2], Ayşe UZGÖREN BARAN[2]

[1]Department of Chemistry, Faculty of Arts and Sciences, Gaziantep University, Gaziantep, Turkey
[2]Department of Chemistry, Faculty of Science, Hacettepe University, Ankara, Turkey

Received: 03.02.2014 • **Accepted:** 15.07.2014 • **Published Online:** 23.01.2015 • **Printed:** 20.02.2015

Abstract: A series of N-acylhydrazone derivatives (**2a**–**2p**) containing 6-methoxy-naphthalene and acylhydrazone moieties were synthesized in good yield using microwave irradiation and developed as potential COX-2 inhibitors. Furthermore, the interactions between COX-2 and the compounds were examined in detail by molecular modeling studies such as structure–activity relationship and molecular docking performed using Gaussian 09 and Discovery Studio 3.5. As a result, it was found that N-acylhydrazone compounds displayed a different mechanism than SC-558 as COX-2 inhibitor by binding to different active sites of the protein, COX-2. Compound **2c** would be a good COX-2 inhibitor candidate for preclinical studies.

Key words: Naproxen, microwave, acyl hydrazones, molecular docking

1. Introduction

Nonsteroidal anti-inflammatory drugs (NSAIDs) are used to reduce pain, inflammation, and fever. Most NSAIDs reduce pain by preventing prostaglandin biosynthesis, by inhibiting the activity of the cyclooxygenase enzyme (COX).[1] Until 1990, only one form of the COX enzyme was known and it was thought to be responsible for both its anti-inflammatory activity and unwanted side effects. After 1990, it was found that the COX enzyme had 2 iso forms: COX-1 (constitutive form) and COX-2 (inducible form). Inhibition of the COX-1 enzyme causes some of the unwanted side effects such as gastrointestinal hemorrhage, ulceration, and decreased renal function, while inhibition of COX-2 is responsible for reducing pain, fever, etc.[2] An ideal NSAID would inhibit COX-2 enzyme activity without affecting COX-1 enzyme activity. To find an ideal NSAID, researchers synthesized many COX-2 selective hybrid NSAID compounds. Unfortunately, at the end of 2004, the COX-2 selective NSAID drug rofecoxib was withdrawn from the market because it was discovered that it increased the risk of cardiovascular events.[3]

After that many new studies were conducted to find NSAIDs that were safe in both gastrointestinal and cardiovascular terms. In these studies, naproxen showed the lowest cardiovascular risk[4,5] but had significant gastrointestinal side effects.[6–8] As part of the research, molecular modeling techniques[9] were used to design and develop the optimal compound(s) with less time, labor, and cost. Such methods also became increasingly useful in many other clinically oriented studies.[10]

In the present study, we planned to synthesize hybrid compounds of naproxen that minimize the side

*Correspondence: ttaskin@gantep.edu.tr

effects of NSAIDs[11] according to the literature.[6–8] In addition, in the literature acyl hydrazone derivatives of naproxen have shown cytotoxic activity against a human prostate cancer (Pc-3) cell line in vitro.[12] These compounds were synthesized with higher yields, less reaction time, and in an environmentally friendly manner. Additionally, molecular modeling techniques were applied to identify the site of ligand binding and the geometry of the complex.

2. Results and discussion

The synthetic route used to synthesize naproxen-based acylhyrazone derivatives is outlined in the Scheme. The starting compound, 2-(6-methoxy-naphthalen-2-yl)-propionic acid hydrazide (**1**), was prepared according to the published procedure.[12]

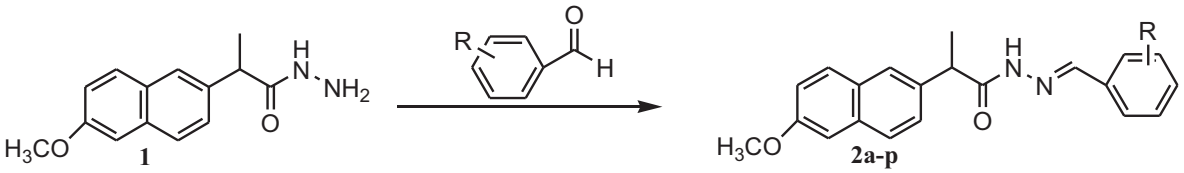

Scheme. Synthetic route of naproxen-based acylhyrazone derivatives (R: H, F,Cl, Br, CH_3 and OCH_3).

In the present study, naproxen-based acylhydrazone derivatives were synthesized using both conventional and microwave-assisted methods. Detailed information on these methods is given in the Experimental section. For the microwave-assisted method, the reaction of hydrazide **1** with benzaldehyde was carried out at 50 W, 100 W, 200 W, and 300 W for 2 min in the synthesis of **2a** to optimize the reaction of microwave irradiation (MWI) power. The obtained results showed that the yield of product **2a** was improved as the MWI power increased from 50 W to 200 W but as the MWI power continued to increase the yield of the products decreased. Consequently, 200 W was used for synthesizing all the others (Figure 1).

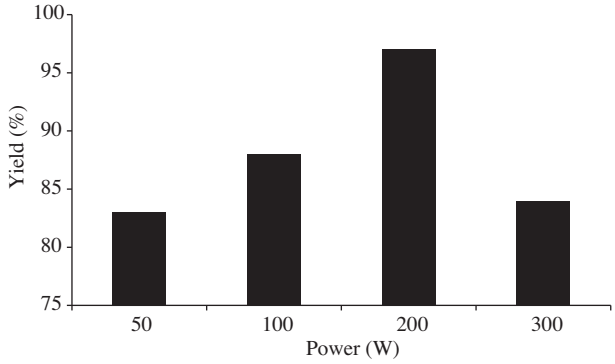

Figure 1. Effect of MWI power on the yield of compound **2a**.

The results showed that the yield of all the products in the microwave-assisted method was higher compared to the yield obtained by synthesis using the conventional technique. A comparative study in terms of reaction time and yield is shown in Table 1. The yield and time data for compounds **2a**, **2b**, **2d**, **2g**, and **2m** are taken from the literature.[12] The melting points, molecular formulae, and weights of the synthesized compounds are also given in Table 1.

The synthesized compounds were also characterized by IR, ^{1}H NMR, and APT-NMR spectra.

Table 1. Molecular formula, molecular weight, melting points, reaction yields, and formulae of the compounds synthesized.

Entry	R	Molecular formula	Molecular weight (g/mol)	Time (min)		Yield (%)		Melting point (°C)
				CH	MW	CH	MW	
2a	H	$C_{21}H_{20}N_2O_2$	308.42	300[a]	2	80[a]	97	134.0–136.0
2b	2-Cl	$C_{21}H_{19}ClN_2O_2$	342.86	300[a]	2	78[a]	87	164.5–165.1
2c	3-Cl	$C_{21}H_{19}ClN_2O_2$	342.86	120	2	83	92	167.8–168.9
2d	4-Cl	$C_{21}H_{19}ClN_2O_2$	342.86	300[a]	2	69[a]	70	170.6–171.3
2e	2-Br	$C_{21}H_{19}BrN_2O_2$	387.31	120	2	62	81	173.1–173.8
2f	3-Br	$C_{21}H_{19}BrN_2O_2$	387.31	120	2	76	80	178.1–179.7
2g	4-Br	$C_{21}H_{19}BrN_2O_2$	387.31	300[a]	2	84[a]	85	174.1–175.6
2h	2-F	$C_{21}H_{19}FN_2O_2$	326.41	120	2	84	96	151.9–153.6
2i	3-F	$C_{21}H_{19}FN_2O_2$	326.41	120	2	72	93	171.2–173.6
2j	4-F	$C_{21}H_{19}FN_2O_2$	326.41	180	2	81	87	175.2–176.6
2k	2-OCH_3	$C_{22}H_{22}N_2O_3$	338.44	120	2	84	87	162.5–163.2
2l	3-OCH_3	$C_{22}H_{22}N_2O_3$	338.44	120	2	63	66	162.5–163.0
2m	4-OCH_3	$C_{22}H_{22}N_2O_3$	338.44	300[a]	2	75[a]	85	146.8–147.9
2n	2-CH_3	$C_{22}H_{22}N_2O_2$	322.44	120	2	82	85	161.6–162.5
2o	3-CH_3	$C_{22}H_{22}N_2O_2$	322.44	120	2	85	89	174.5–175.7
2p	4-CH_3	$C_{22}H_{22}N_2O_2$	322.44	120	2	75	82	158.1–159.2

[a]These data are taken from the literature.[12]

In the IR spectra of compounds **2a**–**p**, the N–H, C=O, and C=N bands were observed in the 3184–3154 cm^{-1}, 1687–1646 cm^{-1}, and 1611–1593 cm^{-1} regions, respectively.

In agreement with the literature data, all groups exhibited 2 sets of signals in the ^{1}H NMR spectrum of compounds **2a**–**p**.[13,14] An azomethine (CH=N) group proton appeared at δ values between 8.15 and 8.54 ppm as a singlet. The amide protons (CONH) appearing as singlets resonated at δ values between 11.53 and 11.86 ppm. Furthermore, the protons of CONH and CH=N exhibited 2 separate signals in ^{1}H NMR spectra at 11.23–11.54 ppm and 7.85–8.26 ppm respectively, due to the nitrogen inversion and 2 conformers (E/Z) of each structure. The other protons were observed according to the expected chemical shift and integral values.

In the APT-NMR spectra of compound **2a**–**2p**, the carbon signal due to –CHO was observed at δ values between 174.91 and 175.69 ppm. The chemical shift of amidic carbonyl groups of the other form was exhibited at δ values between 169.77 and 170.66 ppm. The other carbons were observed according to the expected chemical shifts.

In order to obtain information about the electronic structures and 3D geometries of naproxen-based acylhyrazone derivatives (Table 1), molecular modeling techniques were also implemented. In the present study, we used 2 methods: structure–activity relationship (SAR) and molecular docking. Before these applications, we prepared the target compounds (**2a**–**2p**). First of all, the target compounds were optimized using semi-empirical/PM3 and DFT/B3LYP/6-31G* levels as implemented in G09,[15] because they were mostly used in molecular modeling techniques. The conformations of these compounds were subsequently computed using conformation search and minimization of DS 3.5[16] using the CHARMm.[17] The conformational analysis reported the 2 most stable conformers, which are shown only for compound **2a** as template (Figure 2). Moreover, the absolute energy values for each conformer of all compounds are listed in Figure 3.

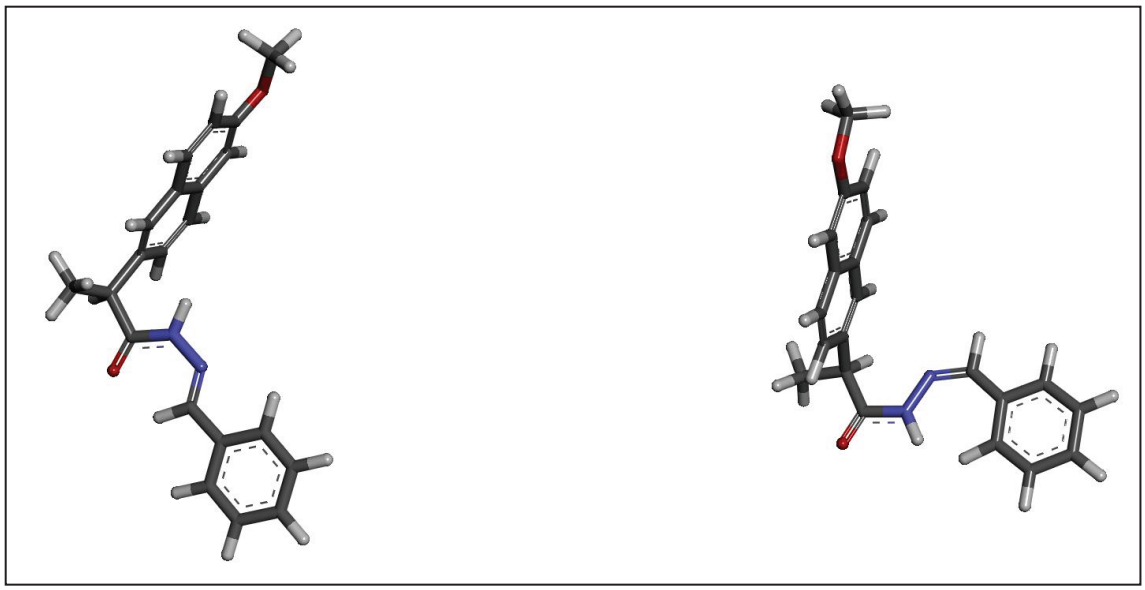

Figure 2. Structure of the E/E (left) and Z/Z (right) conformers of **2a**.

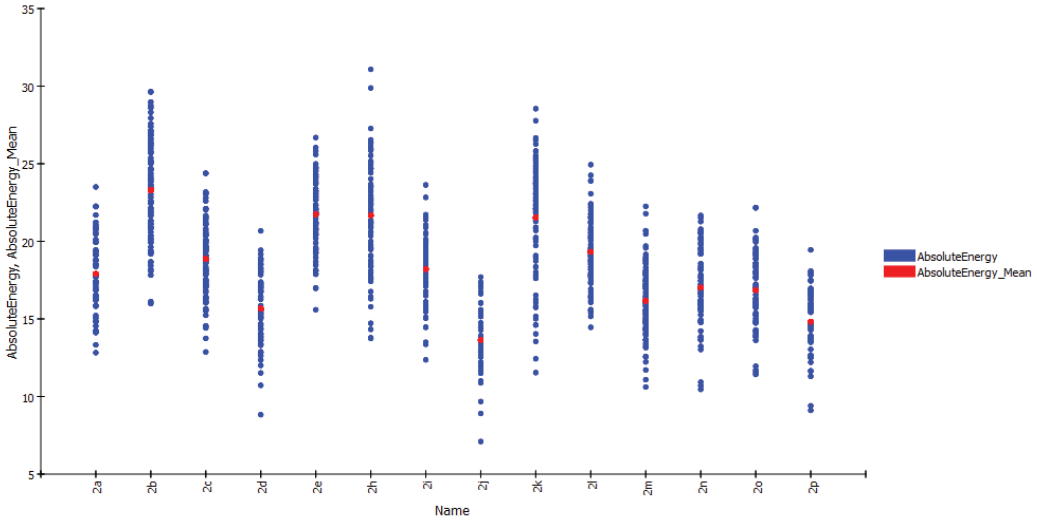

Figure 3. The absolute energy values for each conformer of all compounds.

It is known that a structure–activity relationship study is a good method to predict various biological activities using quantum chemical descriptors[18–21] in the absence of experimental data. In particular, net atomic charges, HOMO–LUMO energies, frontier orbital electron densities, and superdelocalizabilities have been used to correlate with various biological activities.[22] In addition, Parr et al.[18] have defined a new descriptor, electrophilicity index, which was applied for prediction of various biological activities of chemical compounds. Maynard et al.[19] have also mentioned that electrophilicity index is directly correlated with the ability to identify the function or capacity of an electrophile and the electrophilic power of the inhibitors. Moreover, previous studies[21,23–24] confirmed electrophilicity index as a possible descriptor of biological activity for different chemical structures. In the present study, we focused on the quantum chemical descriptors of the investigated compounds, because these descriptors helped us to achieve a deeper understanding of the structure

Table 2. Density functional and semi-empirical theories based descriptors of the E/E/trans conformer of 2a–2p in G09.

DFT	Comp.	(D)	HOMO (eV)	LUMO (eV)	(IP)	(EA)	(η)	(S)	(χ)	(θ)	(ω)
1	**2a**	4.058	–5.625	–1.274	5.62541	1.27431	2.17555	0.45965	–3.44986	3.44986	2.73529
2	**2b**	5.465	–5.665	–1.443	5.66460	1.44329	2.11065	0.47379	–3.55394	3.55394	2.99209
3	**2c***	6.259	–5.699	–1.471	5.69888	1.47050	2.11419	0.47299	–3.58469	3.58469	3.03900
4	**2d**	5.394	–5.691	–1.450	5.69072	1.44955	2.12058	0.47157	–3.57014	3.57014	3.00527
5	**2e**	5.398	–5.663	–1.441	5.66296	1.44084	2.11106	0.47370	–3.55190	3.55190	2.98808
6	**2f***	6.143	–5.697	–1.469	5.69671	1.46914	2.11378	0.47309	–3.58292	3.58292	3.03658
7	**2g**	5.340	–5.691	–1.458	5.69072	1.45771	2.11650	0.47248	–3.57422	3.57422	3.01796
8	**2h**	4.914	–5.641	–1.358	5.64120	1.35812	2.14154	0.46695	–3.49966	3.49966	2.85954
9	**2i***	5.629	–5.677	–1.397	5.67739	1.39676	2.14031	0.46722	–3.53707	3.53707	2.92268
10	**2j**	4.772	–5.658	–1.314	5.65779	1.31431	2.17174	0.46046	–3.48605	3.48605	2.79788
11	**2k**	2.477	–5.506	–1.186	5.50595	1.18560	2.16018	0.46293	–3.34578	3.34578	2.59104
12	**2l**	3.862	–5.603	–1.236	5.60337	1.23567	2.18385	0.45791	–3.41952	3.41952	2.67718
13	**2m**	2.547	–5.434	–1.184	5.43357	1.18424	2.12467	0.47066	–3.30891	3.30891	2.57661
14	**2n**	3.857	–5.621	–1.279	5.62106	1.27894	2.17106	0.46060	–3.45000	3.45000	2.74117
15	**2o**	3.693	–5.613	–1.246	5.61290	1.24574	2.18358	0.45796	–3.42932	3.42932	2.69288
16	**2p**	3.877	–5.604	–1.237	5.60392	1.23676	2.18358	0.45796	–3.42034	3.42034	2.67879
Std.	**NS-398**	5.577	–6.452	–2.359	6.45209	2.35896	2.04657	0.48862	–4.40553	4.40553	4.74175
Std.	**SC-558**	5.009	–6.707	–1.800	6.70734	1.79976	2.45379	0.40753	–4.25355	4.25355	3.68669

Table 2. Continued

PM3	Comp.	(D)	HOMO (eV)	LUMO (eV)	(IP)	(EA)	(η)	(S)	(χ)	(θ)	(ω)
1	**2a**	3.003	−8.774	−0.662	8.77350	0.66205	4.05572	0.24657	−4.71778	4.71778	2.74395
2	**2b**	3.389	−8.792	−0.681	8.79228	0.68137	4.05545	0.24658	−4.73682	4.73682	2.76634
3	**2c***	3.977	−8.807	−0.697	8.80670	0.69661	4.05504	0.24661	−4.75165	4.75165	2.78397
4	**2d**	3.564	−8.803	−0.694	8.80343	0.69389	4.05477	0.24662	−4.74866	4.74866	2.78065
5	**2e**	3.334	−8.795	−0.684	8.79527	0.68437	4.05545	0.24658	−4.73982	4.73982	2.76984
6	**2f***	4.189	−8.815	−0.706	8.81540	0.70559	4.05491	0.24661	−4.76050	4.76050	2.79443
7	**2g**	3.798	−8.816	−0.707	8.81595	0.70668	4.05463	0.24663	−4.76131	4.76131	2.79558
8	**2h**	3.620	−8.799	−0.688	8.79908	0.68790	4.05559	0.24657	−4.74349	4.74349	2.77404
9	**2i***	4.680	−8.824	−0.715	8.82438	0.71512	4.05463	0.24663	−4.76975	4.76975	2.80550
10	**2j**	4.031	−8.817	−0.708	8.81731	0.70804	4.05463	0.24663	−4.76268	4.76268	2.79718
11	**2k**	3.150	−8.747	−0.635	8.74710	0.63539	4.05586	0.24656	−4.69125	4.69125	2.71309
12	**2l**	3.018	−8.783	−0.672	8.78302	0.67239	4.05531	0.24659	−4.72771	4.72771	2.75579
13	**2m**	3.721	−8.751	−0.652	8.75119	0.65171	4.04974	0.24693	−4.70145	4.70145	2.72902
14	**2n**	2.853	−8.770	−0.659	8.76996	0.65879	4.05559	0.24657	−4.71437	4.71437	2.74009
15	**2o**	2.783	−8.767	−0.655	8.76670	0.65498	4.05586	0.24656	−4.71084	4.71084	2.73579
16	**2p**	2.844	−8.763	−0.652	8.76343	0.65171	4.05586	0.24656	−4.70757	4.70757	2.73200
Std.	**NS-398**	4.674	−9.652	−1.123	9.65188	1.12301	4.26443	0.23450	−5.38745	5.38745	3.40310
Std.	**SC-558**	5.467	−10.150	−1.497	10.1495	1.49663	4.32661	0.23113	−5.82324	5.82324	3.91878

*symbol shows the higher biological activities among all compounds. Comp.: compound; D: Molecular dipole moment; I: Ionization potential; EA: Electron affnity; η: Chemical hardness; S: Softness; χ: Electronegativity; θ: Chemical potential; ω: Electrophilicity index; Std: Standard

activity relationship of the compounds without their activity values. The direct and indirect calculated semi-empirical (PM3) and density functional theory (DFT)-based chemical descriptors are shown in Table 2 for the E/E conformer of **2a**–**2p** in G09, due to its being the most stable conformer of the studied compounds. Then we evaluated the calculated data containing PM3- and DFT-based chemical descriptors. Figure 4 shows that both of them have almost the same trends for the investigated compounds, but comparison amongst compounds or evaluation of results obtained by DFT-based chemical descriptors was more pronounced than PM3-based chemical descriptors, because the data obtained by semi-empirical theory-based chemical descriptors values were very close together and inevitably more difficult to examine in comparisons. In this part, we concluded that the calculated data obtained by DFT for the target compounds (**2a**–**2p**) were more accurate and consistent than the others.

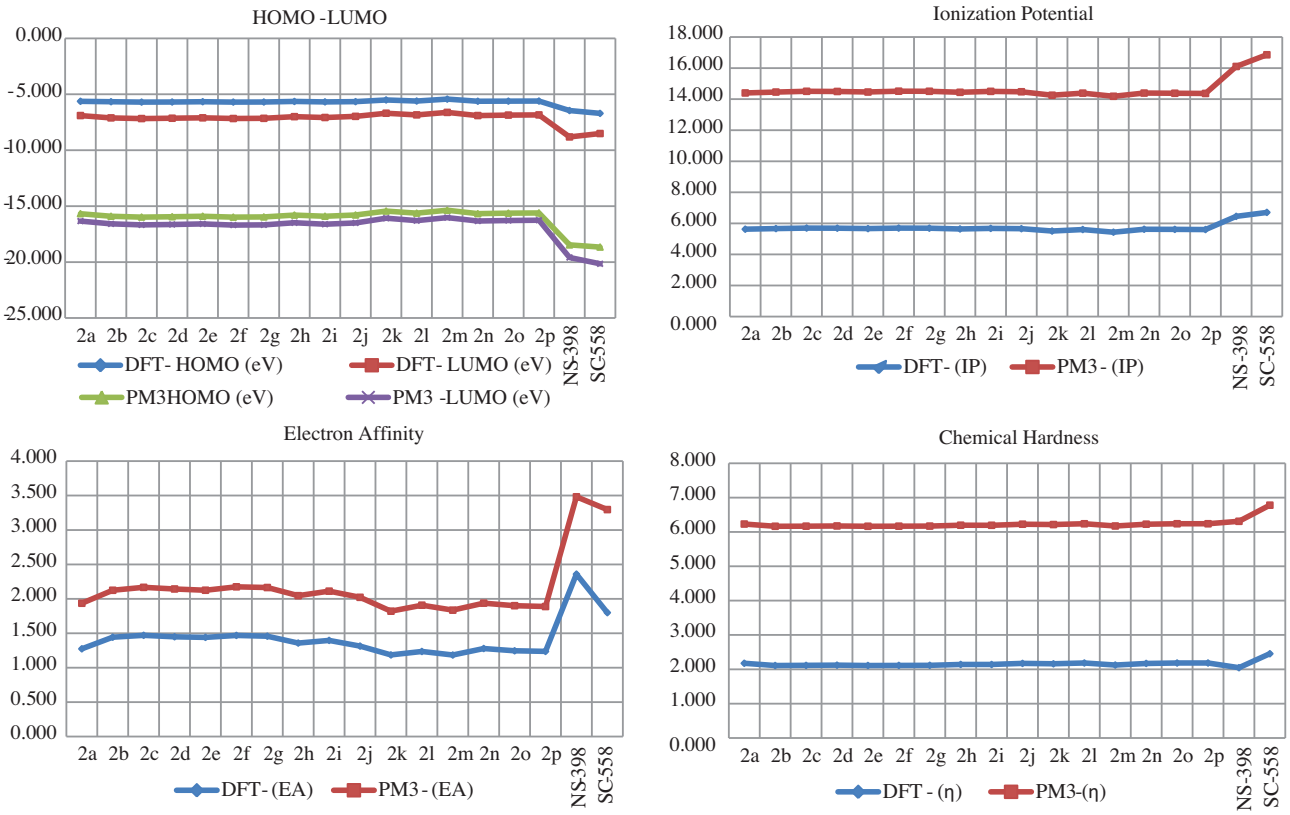

Figure 4. DFT- and PM3-based chemical descriptors of compounds **2a**–**2p**.

After that, SAR results of the compounds (**2a**–**2p**) were explained using DFT-based chemical descriptors. These descriptors provide information about the chemical reactivity (biological activity) and stability of naproxen-based acylhyrazone derivatives. Molecular dipole moment is a measure of net molecular polarity; E_{HOMO}, E_{LUMO} are directly correlated with donating and accepting electronic density of the system, respectively. Ionization potential (IP) and electron affinity (EA) define the susceptibility of the compound towards nucleophilic and electrophilic attack, respectively. IP and EA were also easily obtained from HOMO and LUMO energies. Chemical hardness (η) is directly correlated with the stability of the molecule. The chemical potential (μ) characterizes the escaping tendency of the electron density from the equilibrium state and electrophilicity index (ω) is a measure of the electrophilic power of a molecular towards a nucleophile structure. If the elec-

trophilicity value of a compound was larger than that of other compounds, the mentioned compound has higher reactivity and biological activity than the others.

In the SAR study, **2b**–**2p** were compared with **2a**, which does not have any substituent groups on the benzene ring, and the positive controls, SC-558 and NS-398 compounds, with help of the calculated DFT-based chemical descriptors. Then we interpreted the effect of different substituent groups (–Cl, –Br, –F, $-OCH_3$,

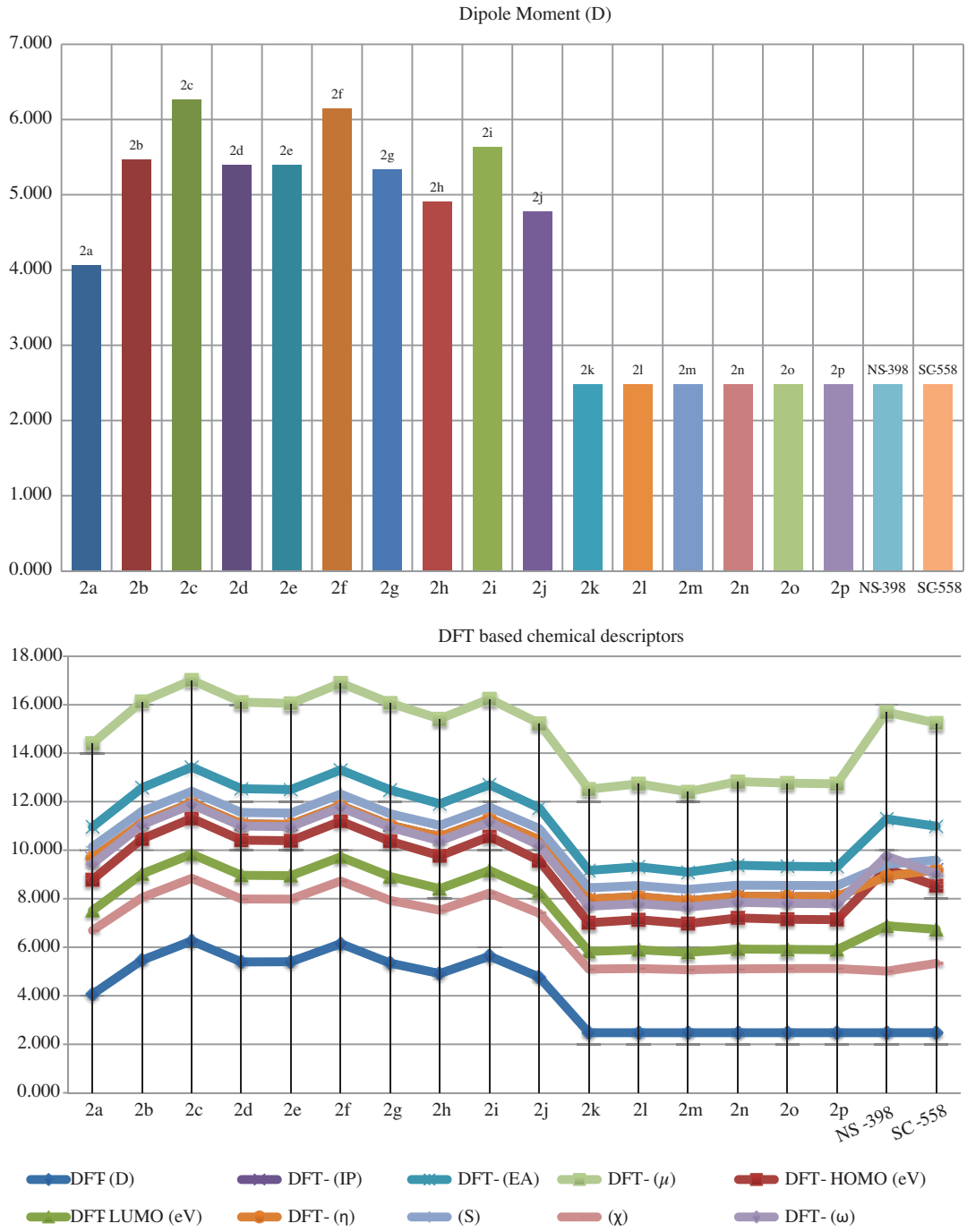

Figure 5. A. The dipole moment values of compounds **2a**–**2p**; B. DFT-based chemical descriptors of compounds **2a**–**2p.**

–CH_3) on different positions of the benzene ring of **2a** and mentioned positive controls. Firstly, molecular dipole moment or molecular polarity values shown in Table 2 were examined. Compounds **2b**–**2j**, including electron-withdrawing groups (–Cl, –Br, –F), were more polar than compounds **2k**–**2p**, containing electron-donor groups (–OCH_3, –CH_3). Compounds **2c**, **2f**, and **2i**, which included halogen atoms on the meta position of the benzene ring, have higher molecular dipole moment values than the others and the positive controls as shown in Figure 5A. It was not sufficient to predict the biological activities of the compounds. In addition, we looked at other calculated descriptors. In parallel with the results of the molecular dipole moment descriptor, the obtained DFT-based descriptors such as ionization potential and electron affinity showed similar trends for all compounds (Figure 5B). As a complement, electrophilicity index (ω) values of the compounds were also evaluated. The electrophilicity index as a possible descriptor of biological activity indicated that the substitution of the –Cl, –Br, and –F groups to the meta position of the benzene ring (compounds **2c**, **2f**, and **2i**, ω: 3.039, 3.037, 2.923) resulted in a remarkable increase in COX-2 inhibitory potency, whereas –OCH_3 or –CH_3 groups showed weak selectivity for COX-2, due to low ω values, for example compounds **2k**, **2m**, and **2p**, ω: 2.591, 2.577, 2.679, respectively. It is interesting to note that compounds ortho and para substituted with electron-withdrawing groups exhibited moderate ω values compared to meta substituted forms of each compound like compounds **2c**, **2f**, and **2i** as shown Figure 6 and Table 2.

On the other hand, electron-donor groups such as –OCH_3 and –CH_3 reduce the ω values in these compounds. In particular, ortho and para substituted forms of compounds **2k**, **2m**, and **2p** exhibited lower ω values.

In summary, the substituents and positions on the benzene ring of the investigated compounds had very important effects on biological activity (Figure 6; Table 2). When the compounds were compared with the

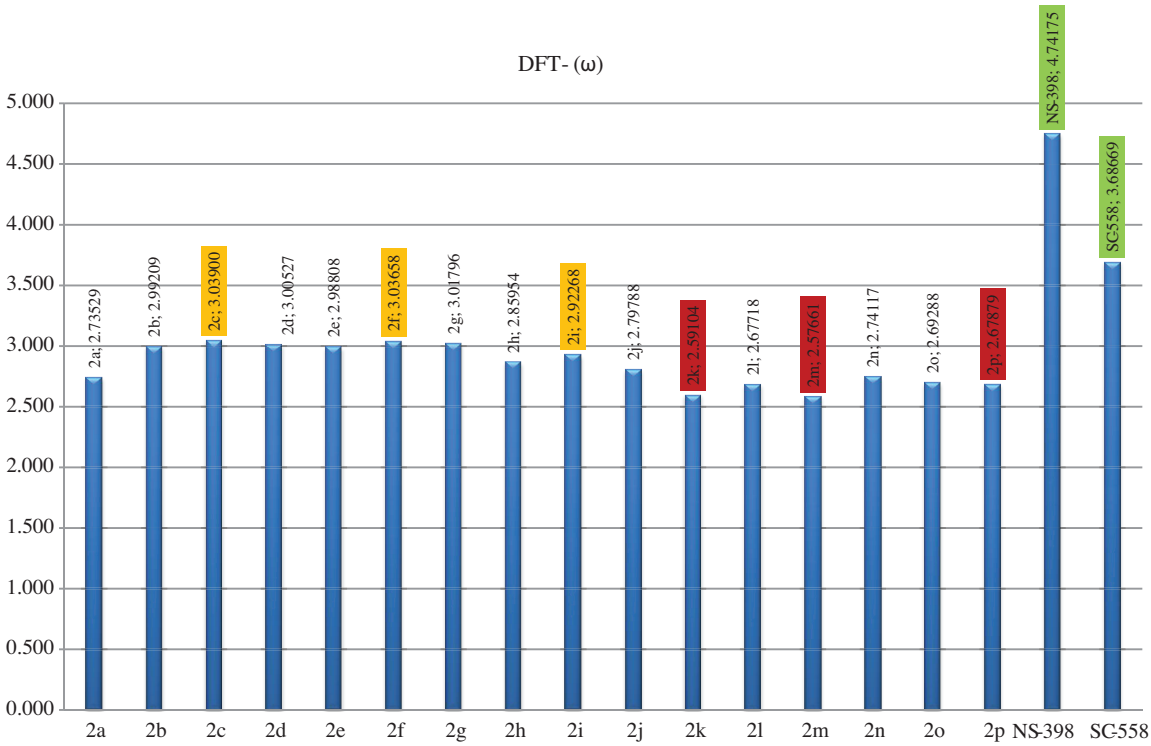

Figure 6. The electrophilicity index values of compounds **2a**–**2p**.

positive controls, SC-558 and NS-398 compounds, none of them were as effective as the positive controls (Figure 6). Therefore, molecular docking was performed to determine why naproxen-based acylhydrazone derivatives showed less activity than SC-558 as standard compound. Moreover, the ligands (compounds **2c**, **2f**, **2i**, **2k**, **2m**, and **2p**), which were chosen based on the results of the SAR study, were docked with the active site of COX-2 to understand their orientations. For comparison of the ligands orientations, we superimposed each compound's best pose, which was obtained by locating the lowest binding energy, the largest minus CDOCKER energy and the lowest minus CDOCKER interaction energy. In addition, root mean square deviation (RMSD) values of each pose were calculated and all RMSD values of the compounds were smaller than 2.0 in DS 3.5 (Table 3). It was shown that SC-558 as standard compound containing the 4-bromobenzylidene moiety fitted into the cavity formed by Leu352,Gln192, Met522, Trp387, Leu384, Phe381, Gly526, Tyr385, Ala527, and Tyr348, while the 3-(trifluoromethyl)-1H-pyrazole moiety fitted into the other cavity formed by Tyr355, Val349, Leu359, Val116,

Table 3. Molecular docking results of the selected compounds (**2c**, **2f**, **2i**, **2k, 2m**, and **2p**).

Name	Binding Eng.	CDOCKER Eng.	CDOCKER Int. Eng.	HBOND-LYS83	HBOND-TYR115	RMSD
2c	–10.8774	–14.3397	33.7329	**1**(1.868 Å)	**1**(2.446 Å)	0
2f	3.448	–13.998	–33.242	**-**	**-**	0
2i	–8.969	–12.435	–31.730	**1** (1.885 Å)	**1** (2.360 Å)	0
2k	–9.599	–11.724	–35.332	**1** (1.822 Å)	**1** (2.334 Å)	0
2m	1.932	–7.2496	–29.318	-	**1** (2.436 Å)	0
2p	–10.020	–13.714	–32.771	**1** (1.872 Å)	**1** (2.320 Å)	0

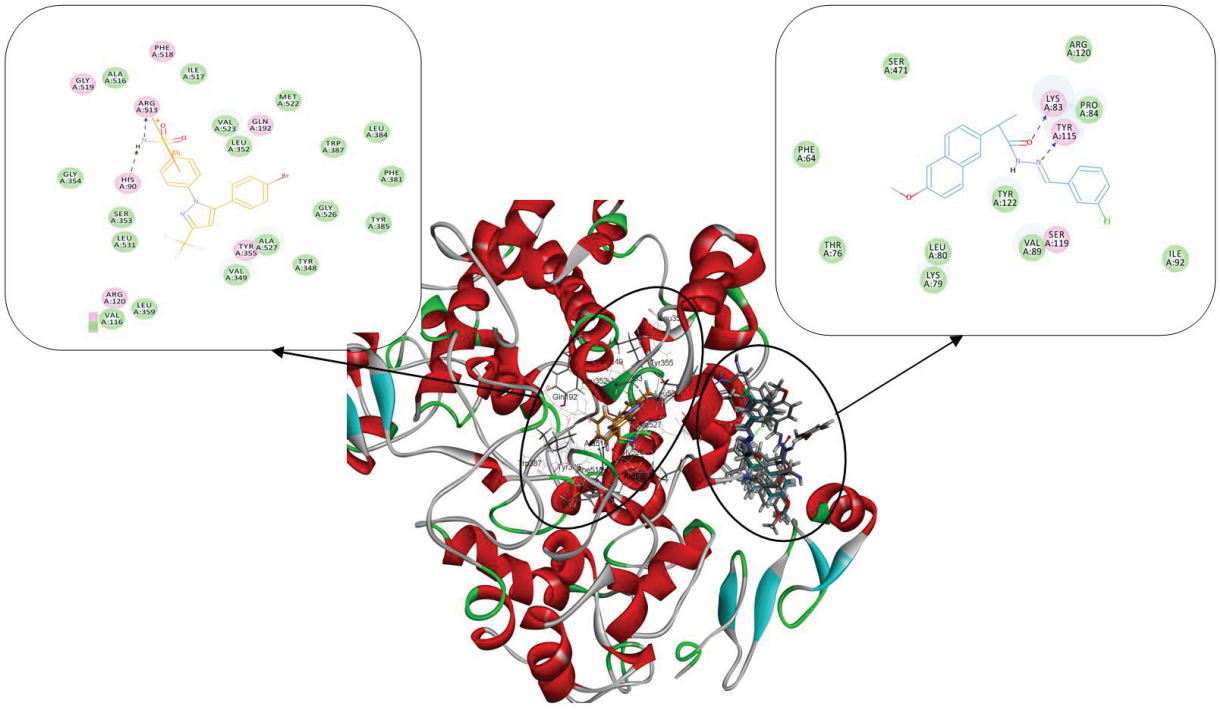

Figure 7. Interactions between the COX-2 and **SC-558** (left) and compound **2c** (right) on a 2D diagram.

Arg120, Leu531, and Ser353 (Figure 7). These features[25] were mentioned and common in COX-2 inhibitors like SC-558. Due to the lowest binding energy value of compound **2c** according to docking results, compound **2c** was the best-docked conformation of the selected compounds. As a result of molecular docking, the OH group of Tyr115 formed a hydrogen bond (2.446 Å) with the N=C moiety of compound **2c**, and the N–H moiety of Lys83 hydrogen bonded (1.868 Å) to the C=O of the hydrazone (Figure 8). When we look at the other selected compounds **2f**, **2i**, **2k**, **2m**, and **2p**, which are base forms of **2c**, their orientations were different from that of compound **2c** in active site of COX-2 (Figures 9A–9F). It was observed that orientations of the compounds that bind the same amino acids of the active site of COX-2 were very important to determine their biological activities in the same active site of COX-2.

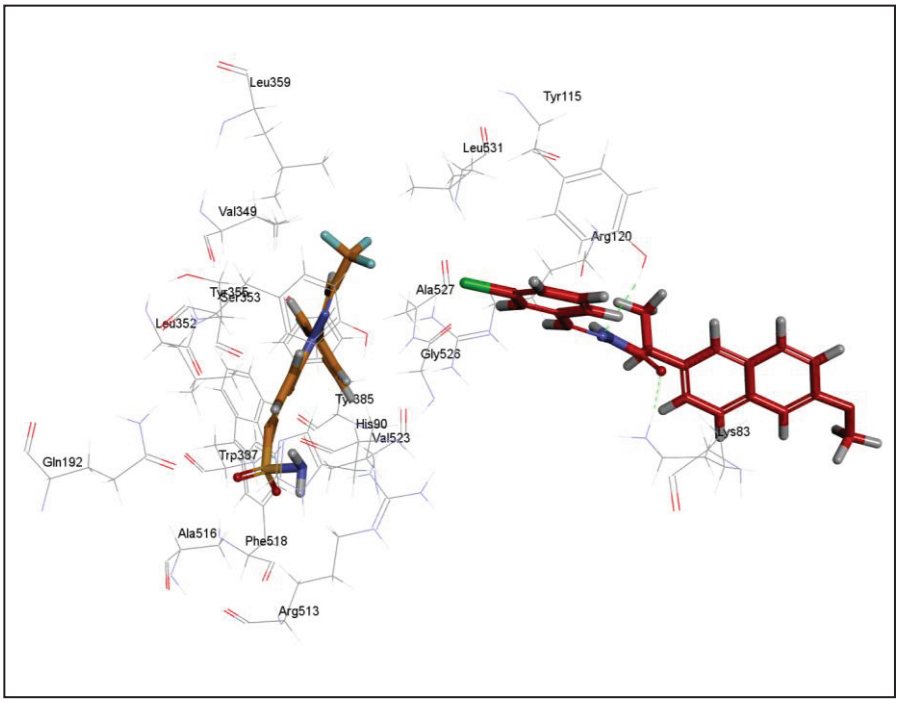

Figure 8. The orientation of **SC-558** and compound **2c** in COX-2 enzyme (**SC-558** is shown in orange and H bonds are shown in green).

Furthermore, we observed the main different active sites of the selected compounds and SC-558. Figures 7 and 8 exhibited active sites of compound **2c** and SC-558, which are located outside and inside the COX-2 surface, respectively. This condition was realized with different selectivity and reactivity of the selected compounds and SC-558 in COX-2. It was observed that the selected compounds (**2a**–**2p**) were at different pockets (active sites) of COX-2, as given in Figure 7. This situation may explain why the compounds did not display significant selective activity as compared to SC-558 against COX-2 enzyme.

In conclusion, a series of N-acylhydrazone derivatives were synthesized by the reaction of naproxen hydrazide with a variety of aromatic aldehydes using conventional and microwave irradiation techniques. To explore the electronic structures and the mechanisms of naproxen-based acylhydrazone derivatives against COX-2, structure–activity relationship was determined and molecular docking was performed in this study.

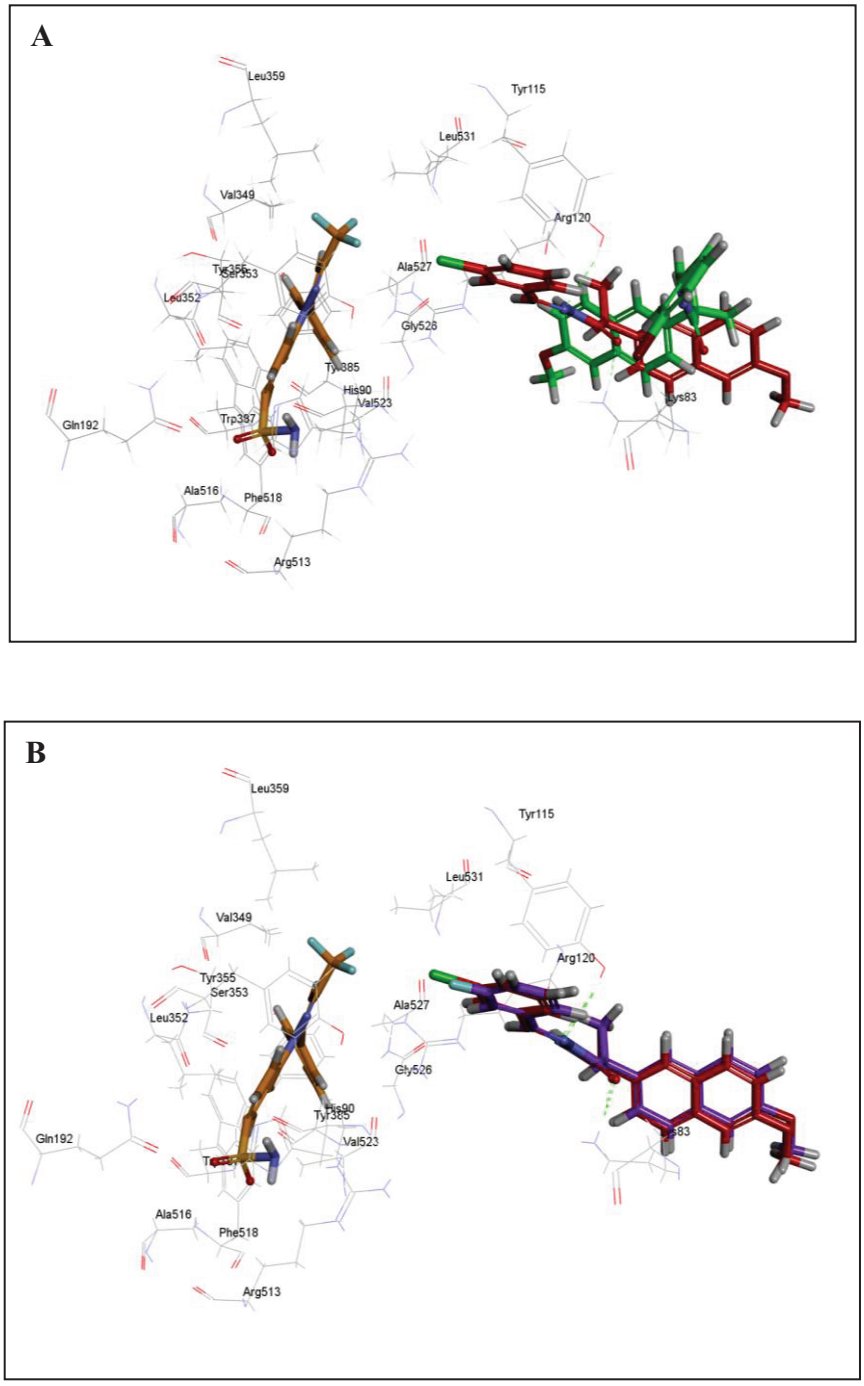

Figure 9. A. The orientation of **SC-558** and compound **2f**; B. The orientation of **SC-558** and compound **2i**, and **2p**) superimposed in COX-2 enzyme. (**SC-558** is shown in orange, the selected compounds (**2c**, **2f, 2i, 2k, 2m**, and **2p**) are shown in red, green, violet, claret red, blue, and pink, respectively; H bonds are shown in green).

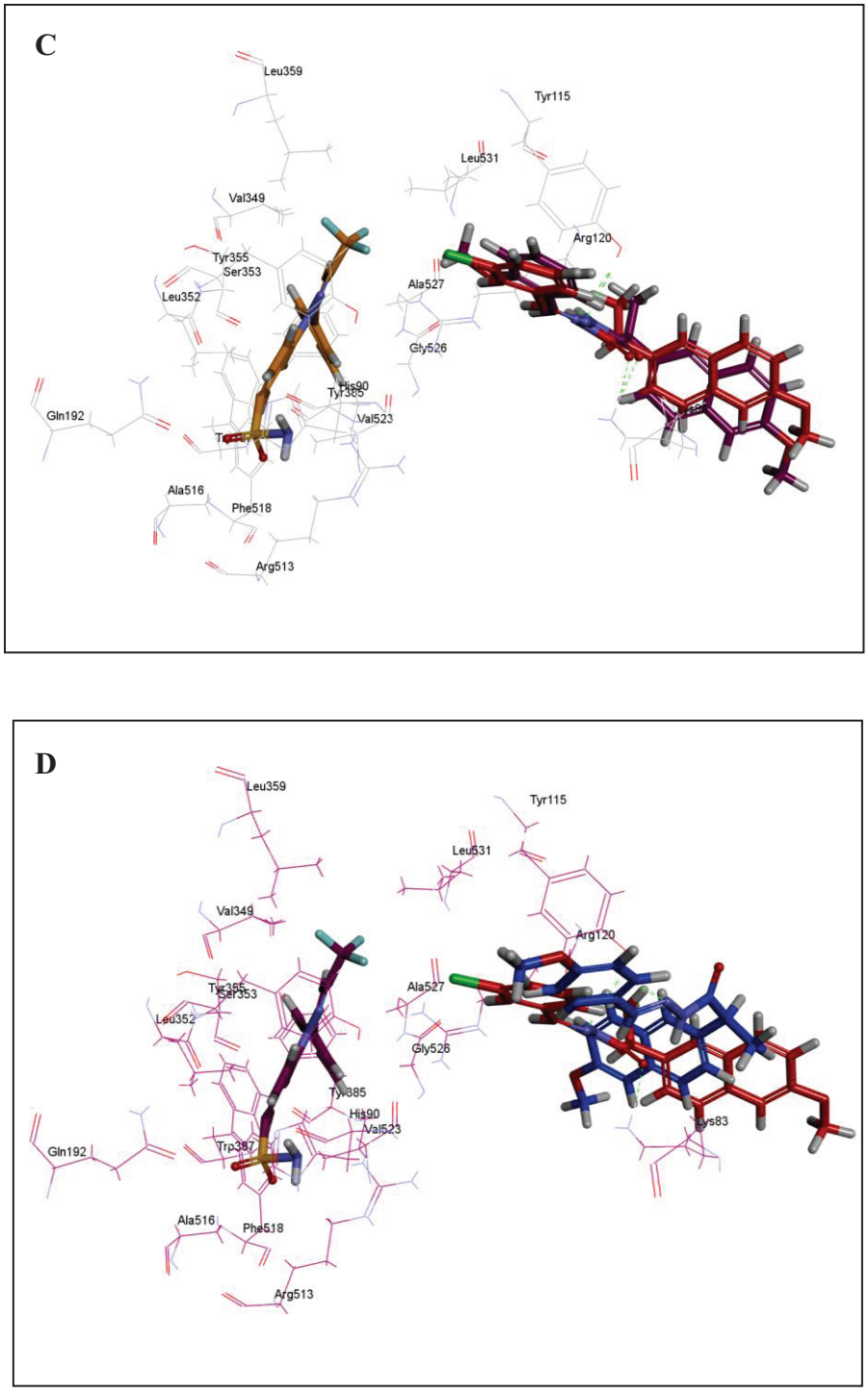

Figure 9. C. The orientation of **SC-558** and compound **2k**; D. The orientation of **SC-558** and compound **2m**, and **2p**) superimposed in COX-2 enzyme. (**SC-558** is shown in orange, the selected compounds (**2c**, **2f, 2i, 2k, 2m**, and **2p**) are shown in red, green, violet, claret red, blue, and pink, respectively; H bonds are shown in green).

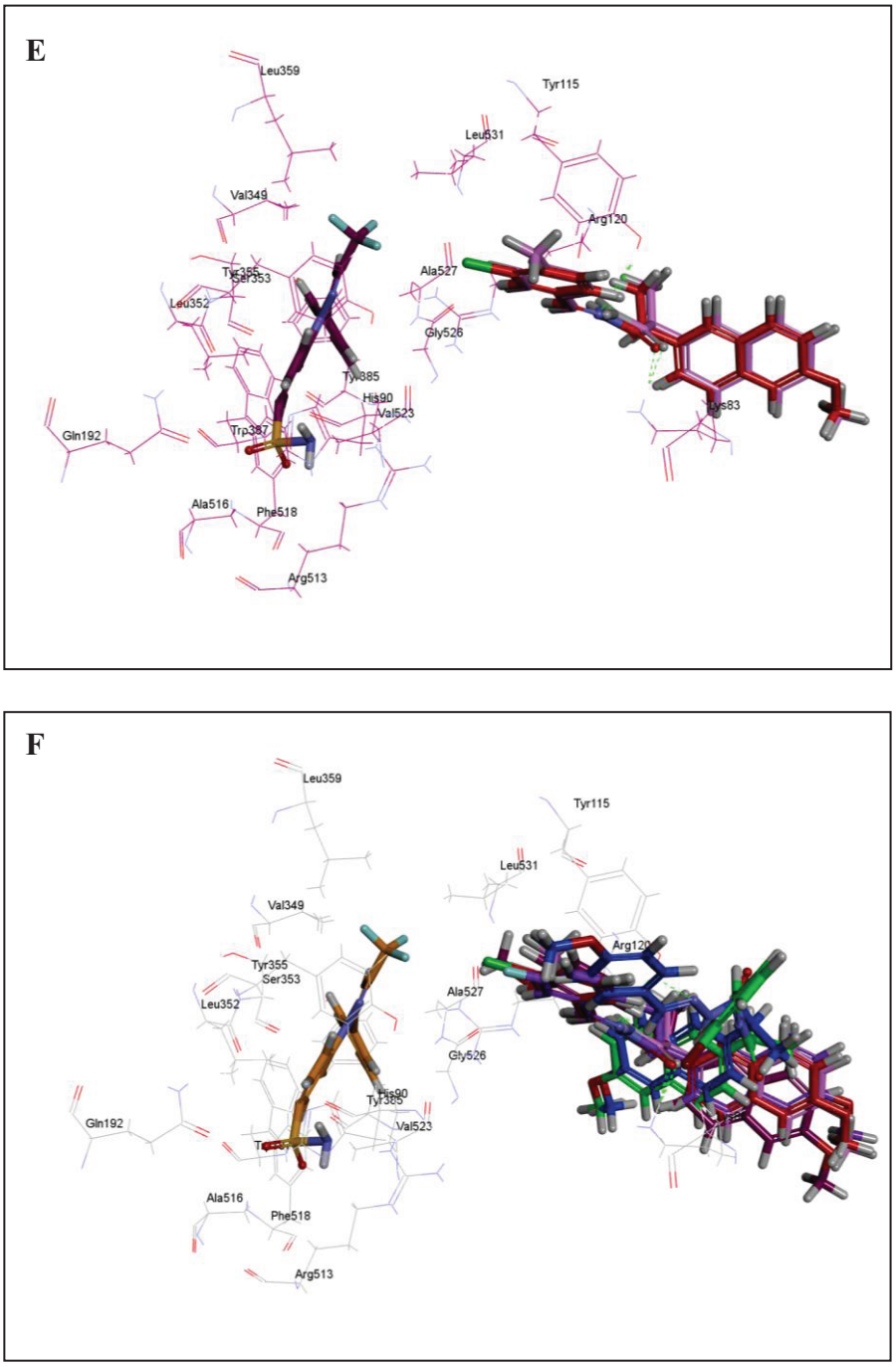

Figure 9. E. The orientation of **SC-558** and compound and **2p** as compared with compound **2c**, which was the best-docked conformation in COX-2 enzyme; F. The orientation of **SC-558** and the selected compounds (**2c, 2f, 2i, 2k, 2m**, and **2p**) superimposed in COX-2 enzyme. (**SC-558** is shown in orange, the selected compounds (**2c**, **2f, 2i, 2k, 2m**, and **2p**) are shown in red, green, violet, claret red, blue, and pink, respectively; H bonds are shown in green).

Based on the synthesis of N-acylhydrazone derivatives, microwave irradiation provided higher yields in a shorter reaction time and in a more environmentally friendly manner than the conventional method. From the results of molecular modeling, it can be concluded that compound **2c** is potential inhibitor of COX-2. Moreover, according to the structure–activity relationship and molecular docking results, it can be stated that N-acylhydrazone derivatives exhibit a totally different mechanism than SC-558 and they bind to a different active site of COX-2. This study reports a deeper insight into the binding of N-acylhydrazone derivatives to COX-2 based on standard compounds. Additionally, the present study will help in the design and development of potent prodrug compounds without undesired effects against COX-2.

3. Experimental

3.1. Chemicals and instrumentation

Naproxen was kindly supplied by Abdi İbrahim Pharmaceuticals. Microwave irradiation was carried out in a microwave oven (Milestone-RotaPREP). All chemicals were from the Aldrich Chemical Co. Melting points were measured in sealed tubes using an electrothermal digital melting point apparatus and are uncorrected. IR spectra (KBr) were recorded on a Thermo Scientific Nicolet iS10 spectrometer. APT and ^{1}H NMR spectra were obtained using a Bruker DPX-400, 400 MHz High Performance Digital FT-NMR Spectrometer using DMSO-d$_6$. All chemical shift values were recorded as δ (ppm). Chemical shift (δ) values of rotameric hydrogens whenever identified are presented within parentheses by assigning an asterisk (*) along with that of other forms. The purity of the compounds was controlled by thin layer chromatography on silica gel-coated aluminum sheets. Compounds **2a**, **2b**, **2d**, **2g**, and **2m** are already recorded in the literature.[12] Conventional synthesis of these compounds was carried out using the reported procedure.[12] Except for compounds **2c** and **2o**, the compounds have CAS Registry Numbers but no reference, analytical, or spectral data; therefore, the analytical and spectral data for the unknown products are described here (Table 1).

3.2. Reactions

3.2.1. Conventional method

To a stirred solution of 2-(6-methoxy-naphthalen-2-yl)-propionic acid hydrazide (**1**) (0.5 g, 2.1 mmol) in ethanol (30 mL) were added various aldehydes (2.1 mmol), after which the mixture was heated at 90–95 °C until completion of the reaction (TLC monitoring). The mixture was cooled to room temperature and the solvent was removed by rotary evaporator. The residue was treated with water. The solid separated was filtered and dried to give the desired products **2a**–**2p**.

3.2.2. Microwave-assisted method

A mixture of 2-(6-methoxy-naphthalen-2-yl)-propionic acid hydrazide (**1**) (0.5 g, 2.1 mmol) and various aldehydes (2.1 mmol) in 3 mL of ethanol was placed in Teflon microwave vessels. The system was heated in a microwave oven for various times at 200 W. After completion of the reaction the residue was treated with water. The solid separated was filtered and dried to give the desired products **2a**–**2p.**

3.3. Characterization data

Schematic structures for **2a**–**2p** are shown in the Scheme; experimental data for **2a**–**2p** are given below.

3.3.1. N′-(3-chlorobenzylidene)-2-(6-methoxynaphthalen-2-yl)propanehydrazide (2c).

White solid, yield 90% (conventional); 96% (microwave), mp 167.8–168.9 °C. IR (ν_{max}, cm^{-1}): 3178, 3040, 2957, 1666 (C=O), 1611 (CN), 1566 cm^{-1}. ^{1}H NMR (400 MHz, DMSO): δ =1.49 (1.46*, 3H, d, J = 7.0 Hz, CH_3), 3.86 (3.84*, 3H, s, OCH_3), 4.76 (1H, q, J = 7.0 Hz, $CHCH_3$), 7.11–7.82 (ArH, m, 10H), 8.17 (7.87*, 1H, s, CH), 11.73 (11.42*, 1H, s, NH). APT-NMR (100 MHz, DMSO): δ = 18.45, 18.54, 41.03, 44.00, 55.04, 55.05, 105.62, 118.60, 118.70, 125.41, 125.50, 125.56, 125.69, 125.87, 126.24, 126.58, 126.75, 126.86, 128.38, 128.45, 128.93, 129.09, 129.20, 129.49, 130.53, 130.55, 133.05, 133.28, 133.57, 133.63, 136.50, 136.53, 137.13, 140.90, 144.94, 156.99, 157.09, 170.11, 175.16. Anal. calcd. for $C_{21}H_{19}ClN_2O_2$: C, 68.76; H, 5.22; N, 7.64. Found: C, 68.37; H, 5.19; N, 7.71.

3.3.2. N′-(2-bromobenzylidene)-2-(6-methoxynaphthalen-2-yl)propanehydrazide (2e).

White solid, yield 68% (conventional); 90% (microwave), mp 173.1–173.8 °C. IR (ν_{max}, cm^{-1}): 3154, 3042, 2969, 2930, 1646 (C=O), 1609 (CN), 1543 cm^{-1}. ^{1}H NMR (400 MHz, DMSO): δ = 1.50 (1.47*, 3H, d, J = 7.0 Hz, CH_3), 3.86 (3.84*, 3H, s, OCH_3), 4.77 (1H, q, J = 7.0 Hz, CH), 7.11–7.99 (ArH, m, 10H), 8.54 (8.26*, 1H, s, CH), 11.86 (11.54*, 1H, s, NH). APT-NMR (100 MHz, DMSO): δ = 19.02, 19.07, 41.50, 44.71, 55.54, 106.13, 119.12, 119.22, 123.73, 123.96, 126.07, 126.24, 126.75, 127.13, 127.28, 127.42, 127.62, 128.36, 128.44, 128.92, 129.00, 129.46, 129.60, 131.66, 131.95, 133.40, 133.46, 133.60, 133.82, 137.02, 137.53, 141.50, 145.33, 157.51, 157.62, 170.66, 175.69. Anal. calcd. for $C_{21}H_{19}BrN_2O_2$: C, 61.33; H, 4.66; N, 6.81. Found: C, 61.20; H, 4.721; N, 6.96.

3.3.3. N′-(3-bromobenzylidene)-2-(6-methoxynaphthalen-2-yl)propanehydrazide (2f).

White solid, yield 86% (conventional); 89% (microwave), mp 178.1–179.8 °C. IR (ν_{max}, cm^{-1}): 3331, 3175, 3048, 2986, 2931, 2845, 1660 (C=O), 1600 (CN), 1552 cm^{-1}. ^{1}H NMR (400 MHz, DMSO): δ = 1.49 (1.46*, 3H, d, J = 7.0 Hz, CH_3), 3.86 (3.84*, 3H, s, OCH_3), 4.75 (1H, q, J = 7.0 Hz, CH), 7.11–7.82 (ArH, m, 10H), 8.16 (7.85*, 1H, s, CH), 11.72 (11.42*, 1H, s, NH). APT-NMR (100 MHz, DMSO): δ = 18.98, 19.07, 41.57, 44.49, 55.55, 55.56, 106.12, 119.11, 119.21, 122.58, 122.66, 126.00, 126.20, 126.31, 126.47, 126.75, 127.07, 127.26, 127.36, 128.88, 128.95, 129.26, 129.45, 129.60, 131.29, 131.31, 132.58, 132.86, 133.55, 133.78, 137.04, 137.21, 137.23, 137.64, 141.27, 145.31, 157.20, 157.48, 157.58, 170.60, 175.63. Anal. calcd. for $C_{21}H_{19}BrN_2O_2$: C, 61.33; H, 4.66; N, 6.81. Found: C, 61.17; H, 4.76; N, 6.88.

3.3.4. N′-(2-fluorobenzylidene)-2-(6-methoxynaphthalen-2-yl)propanehydrazide (2h).

White solid, yield 89% (conventional); 92% (microwave), mp 151.9–153.6 °C. IR (ν_{max}, cm^{-1}): 3184, 3060, 3010, 2928, 1658 (C=O), 1603 (CN), 1562 cm^{-1}. ^{1}H NMR (400 MHz, DMSO): δ = 1.49 (1.47*, 3H, d, J = 7.1 Hz, CH_3), 3.86 (3.84*, 3H, s, OCH_3), 4.78 (3.82*, 1H, q, J = 7.0 Hz, CH), 7.11–7.96 (ArH, m, 10H), 8.43 (8.12*, 1H, s, CH), 11.74 (11.44*, 1H, s, NH). APT-NMR (100 MHz, DMSO): δ 18.92, 18.97, 41.34, 44.61, 55.53, 106.08, 116.29, 116.50, 119.10, 119.21, 122.25, 122.35, 125.32, 126.01, 126.21, 126.63, 126.73, 127.17, 127.24, 127.37, 128.88, 128.95, 129.47, 129.61, 131.91, 132.00, 132.23, 132.32, 133.58, 133.78, 135.92, 136.98, 137.50, 139.78, 157.49, 157.59, 159.81, 159.92, 162.29, 162.40, 170.47, 175.62. Anal. calcd. for $C_{21}H_{19}FN_2O_2$: C, 71.99; H, 5.47; N, 7.99. Found: C, 71.08; H, 5.60; N, 7.98.

3.3.5. N′-(3-fluorobenzylidene)-2-(6-methoxynaphthalen-2-yl)propanehydrazide (2i).

White solid, yield 79% (conventional); 86% (microwave), mp 171.2–173.6 °C. IR (ν_{max}, cm^{-1}): 3166, 3046, 2951, 2898, 1652 (C=O), 1608 (CN), 1552 cm^{-1}. ^{1}H NMR (400 MHz, DMSO): δ = 1.49 (1.47*, 3H, d, J = 7.0 Hz, CH_3), 3.86 (3.84*, 3H, s, OCH_3), 4.78 (1H, q, J = 7.0 Hz, CH), 7.11–7.83 (ArH, m, 10H), 8.20 (7.90*, 1H, s, CH), 11.70 (11.42*, 1H, s, NH). APT-NMR (100 MHz, DMSO): δ = 18.44, 18.54, 40.94, 44.03, 55.00, 55.02, 105.60, 112.42, 112.64, 112.81, 113.03, 116.20, 116.41, 116.48, 116.69, 118.60, 118.70, 123.13, 123.27, 125.51, 125.67, 126.25, 126.66, 126.73, 126.86, 128.40, 128.47, 128.92, 129.09, 130.65, 130.69, 130.73, 130.77, 133.07, 133.29, 136.56, 136.83, 136.88, 136.91, 137.14, 141.18, 145.27, 156.99, 157.10, 161.13, 161.20, 163.55, 163.62, 170.11, 175.19. Anal. calcd. for $C_{21}H_{19}FN_2O_2$: C, 71.99; H, 5.47; N, 7.99. Found: C, 71.27; H, 5.56; N, 7.93.

3.3.6. N′-(4-fluorobenzylidene)-2-(6-methoxynaphthalen-2-yl)propanehydrazide (2j).

White solid, yield 79% (conventional; 83% (microwave), mp 175.2–177.6 °C. IR (ν_{max}, cm^{-1}): 3249, 3066, 2954, 2895, 1658 (C=O), 1608 (CN), 1552 cm^{-1}. ^{1}H NMR (400 MHz, DMSO): δ = 1.49 (1.47*, 3H, d, J = 7.1 Hz, CH_3), 3.86 (3.84*, 3H, s, OCH_3), 4.77 (3.82*, 1H, q, J = 7.0 Hz, CH), 7.11–7.87 (ArH, m, 10H), 8.20 (7.90*, 1H, s, CH), 11.60 (11.32*, 1H, s, NH). APT-NMR (100 MHz, DMSO): δ = 18.45, 18.46, 40.81, 43.98, 55.02, 55.04, 105.59, 105.61, 115.64, 115.68, 115.85, 115.89, 118.59, 118.69, 125.47, 125.70, 126.27, 126.71, 126.83, 128.38, 128.46, 128.73, 128.82, 128.98, 129.04, 129.09, 129.13, 130.82, 130.85, 130.87, 130.90, 133.07, 133.27, 136.64, 137.11, 141.42, 145.51, 156.98, 157.08, 161.60, 161.78, 164.06, 164.24, 169.93, 175.03. Anal. calcd. for $C_{21}H_{19}FN_2O_2$: C, 71.99; H, 5.47; N, 7.99. Found: C, 71.34; H, 5.67; N, 7.86.

3.3.7. N′-(2-methoxybenzylidene)-2-(6-methoxynaphthalen-2-yl)propanehydrazide (2k).

White solid, yield 92% (conventional); 95% (microwave), mp 162.5–163.2 °C. IR (ν_{max}, cm^{-1}): 3316, 3178, 3060, 2975, 2945, 2845, 1666 (C=O), 1602 (CN), 1563 cm^{-1}. ^{1}H NMR (400 MHz, DMSO): δ = 1.48 (1.46*, 3H, d, J = 7.2 Hz, CH_3), 3.83 (3.80*, 3H, s, OCH_3), 3.86 (3.84*, 3H, s, OCH_3), 4.77 (3.78*, 1H, q, J = 7.1 Hz, CH), 7.86–7.00 (ArH, m, 10H), 8.54 (8.24*, 1H, s, CH), 11.59 (11.27*, 1H, s, NH). APT-NMR (100 MHz, DMSO): δ 18.88, 18.97, 41.28, 44.48, 55.57, 56.03, 56.07, 106.13, 112.19, 119.07, 119.17, 121.16, 121.21, 122.61, 122.77, 125.71, 125.83, 125.94, 126.16, 126.77, 127.16, 127.23, 127.29, 128.86, 128.92, 129.47, 129.61, 131.58, 131.89, 133.53, 134.74, 137.17, 137.67, 138.67, 142.44, 157.45, 157.55, 157.95, 158.08, 170.13, 175.40. Anal. calcd. for $C_{22}H_{22}N_2O_3$: C, 72.91; H, 6.12; N, 7.73. Found: C, 72.29; H, 6.12; N, 8.02.

3.3.8. N′-(3-methoxybenzylidene)-2-(6-methoxynaphthalen-2-yl)propanehydrazide (2l).

White solid, yield 75% (conventional); 69% (microwave), mp 162.5–163.0 °C. IR (ν_{max}, cm^{-1}): 3163, 3040, 2933, 2839, 1664 (C=O), 1610 (CN), 1546 cm^{-1}. ^{1}H NMR (400 MHz, DMSO): δ = 1.49 (1.46*, 3H, d, J = 7.1 Hz, CH_3), 3.82 (3.78*, 3H, s, OCH_3), 3.86 (3.84*, 3H, s, OCH_3), 4.76 (1H, q, J = 7.0 Hz, CH), 7.11–7.82 (ArH, m, 10H), 8.17 (7.86*, 1H, s, CH), 11.60 (11.32*, 1H, s, NH). APT-NMR (100 MHz, DMSO): δ = 18.43, 18.63, 40.97, 43.93, 55.07, 55.09, 105.63, 110.71, 111.07, 115.85, 116.05, 118.60, 118.69, 119.54, 119.90, 125.43, 125.47, 126.26, 126.72, 126.76, 126.81, 128.35, 128.43, 128.93, 129.10, 129.83, 129.87, 133.03, 133.24, 135.64, 135.68, 136.60, 137.28, 142.33, 146.50, 156.95, 157.06, 159.45, 169.88, 175.0. Anal. calcd. for $C_{22}H_{22}N_2O_3$: C, 72.91; H, 6.12; N, 7.73. Found: C, 72.54; H, 6.04; N, 7.93.

3.3.9. N′-(2-methylbenzylidene)-2-(6-methoxynaphthalen-2-yl)propanehydrazide (2n).

White solid, yield 90% (conventional); 95% (microwave), mp 161.6–162.5 °C. IR (ν_{max}, cm^{-1}): 3334, 3184, 3057, 2989, 2942, 2854, 1655 (C=O), 1603, 1551 cm^{-1}. ^{1}H NMR (400 MHz, DMSO): δ = 1.49 (1.47*, 3H, d, J = 7.2 Hz, CH_3), 2.39 (2.35*, 3H, s, OCH_3), 3.86 (3.84*, 3H, s, OCH_3), 4.77 (3.82*, 1H, q, J = 7.0 Hz, CH), 7.11–7.82 (ArH, m, 10H), 8.45 (8.20*, 1H, s, CH), 11.55 (11.23*, 1H, s, NH). APT-NMR (100 MHz, DMSO): δ = 19.04, 19.08, 19.44, 19.69, 24.95, 25.80, 33.85, 41.31, 44.56, 48.02, 55.57, 106.13, 119.07, 119.18, 125.98, 126.14, 126.23, 126.41, 126.57, 126.65, 126.78, 127.20, 127.33, 127.81, 128.88, 128.94, 129.48, 129.60, 129.80, 130.06, 131.26, 131.31, 132.66, 133.57, 133.77, 136.88, 137.15, 137.19, 137.58, 142.19, 145.53, 157.48, 157.58, 160.41, 170.22, 175.40. Anal. calcd. for $C_{22}H_{22}N_2O_2$: C, 76.28; H, 6.40; N, 8.09. Found: C, 74.56; H, 7.01; N, 8.58.

3.3.10. N′-(3-methylbenzylidene)-2-(6-methoxynaphthalen-2-yl)propanehydrazide (2o).

White solid, yield 93% (conventional); 96% (microwave), mp 174.5–175.7 °C. IR (ν_{max}, cm^{-1}): 3169, 3042, 2933, 2857, 1687 (C=O), 1593 (CN), 1552 cm^{-1}. ^{1}H NMR (400 MHz, DMSO): δ = 1.49 (1.48*, 3H, d, J = 7.2 Hz, CH_3), 2.35 (2.33*, 3H, s, CH_3), 3.86 (3.84*, 3H, s, OCH_3), 4.76 (3.82*, 1H, q, J = 7.0 Hz, CH), 7.11–7.82 (ArH, m, 10H), 8.15 (7.86*, 1H, s, CH), 11.58 (11.29*, 1H, s, NH). APT-NMR (100 MHz, DMSO): δ = 18.99, 21.32, 21.40, 41.38, 44.43, 55.58, 106.12, 119.08, 119.18, 124.47, 124.84, 125.92, 126.22, 126.77, 127.18, 127.31, 127.58, 127.73, 128.85, 128.93, 129.11, 129.16, 129.45, 129.60, 130.83, 131.12, 133.54, 133.74, 134.67, 134.71, 137.15, 137.66, 138.44, 138.46, 143.12, 147.09, 157.45, 157.55, 170.30, 175.45. Anal. calcd. for $C_{22}H_{22}N_2O_2$: C, 76.28; H, 6.40; N, 8.09. Found: C, 75.26; H, 6.62; N, 8.15.

3.3.11. N′-(4-methylbenzylidene)-2-(6-methoxynaphthalen-2-yl)propanehydrazide (2p).

White solid, yield 80% (conventional); 90% (microwave), mp 158.1–159.3 °C. IR (ν_{max}, cm^{-1}): 3331, 3240, 3178, 3013, 2931, 2848, 1672 (C=O), 1611 (CN), 1572 cm^{-1}. ^{1}H NMR (400 MHz, DMSO): δ = 1.48 (1.46*, 3H, d, J = 7.0 Hz, CH_3), 2.51 (2.50*, 3H, s, CH_3), 3.86 (3.84*, 3H, s, OCH_3), 4.77 (3.82*, 1H, q, J = 7.0 Hz, CH), 7.11–7.86 (10H, m, 10H), 8.15 (7.86*, 1H, s, CH), 11.53 (11.24*, 1H, s, NH). APT-NMR (100 MHz, DMSO): δ = 18.44, 20.95, 24.44, 25.28, 33.34, 40.76, 43.93, 47.51, 55.07, 105.61, 118.57, 118.68, 125.43, 125.70, 126.28, 126.64, 126.74, 126.80, 126.93, 128.37, 128.44, 128.97, 129.11, 129.33, 129.38, 131.50, 131.57, 133.05, 133.25, 136.68, 137.13, 139.39, 139.72, 142.64, 146.63, 156.96, 157.06, 169.77, 174.91. Anal. calcd. for $C_{22}H_{22}N_2O_2$: C, 76.28; H, 6.40; N, 8.09. Found: C, 75.12; H, 6.80; N, 8.47.

4. Computation

4.1. Molecular structures and optimization

The structures of all compounds were drawn and optimized using semi-empirical/PM3 and DFT/B3LYP/6-31G* basis set as implemented in Gaussian 09 (G09).[15] The vibrational frequency calculations at the same level of theories were performed to confirm the global minimum energy of each compound. After that, conformational searching of these compounds was carried out using Chemistry at HARvard Macromolecular Mechanics (CHARMm) force field of Discovery Studio (DS) 3.5.[16] CHARMm provides a vast range of functionality for molecular mechanics. It can be also used in diverse areas of research, including protein modeling and structural biology.[17]

4.2. Structure–activity relationship study

A structure–activity relationship (SAR) study was conducted to define and explain how the substituent on the benzene ring affected the chemical reactivity or biological activity based on quantum chemical descriptors. Molecular dipole moment (μ), energies of the highest occupied (HOMO) and lowest unoccupied (LUMO) molecular orbitals (E_{HOMO}, E_{LUMO}), ionization potential (IP), electron affinity (EA), chemical hardness (η), softness, chemical potential (μ), electronegativity (χ). and electrophilicity index (ω), which are named quantum chemical descriptors,[18–21] were computed based on semi-empirical and density functional theories by using Gaussian 09, due to the reliability and versatility of prediction by these descriptors (Table 2). Additionally, SC-558 and NS-398 compounds as COX-2 inhibitors were used for comparison with the investigated compounds. Therefore, we could easily predict whether these compounds were less or more effective than the standard compounds, SC-558 and NS-398, with these descriptors using Gaussian 09.

4.3. Molecular docking

Molecular docking, an effective method to predict whether ligand(s) will interact with a macromolecular target, was performed with Discovery Studio 3.5 to provide an insight into the chosen compounds: **2c**, **2f**, **2i**, **2k**, **2m**, and **2p**. These compounds were determined based on the results of the structure–activity relationship study of the compounds. Subsequently, a standard compound (SC-558) was also compared with these selected compounds in the 3D visualization window of the DS 3.5 program.

Firstly, ligand(s) and enzyme were prepared using G09 and DS 3.5 software for molecular docking study. The naproxen-based acylhydrazone derivatives as ligands (Table 1) were prepared using G09 as described above. The crystal structure of COX-2 (pdb: 1CX2) complexed with 1-phenylsulfonamide-3-trifluoromethyl-5-(4-bromophenyl) pyrazole (SC-558) was downloaded from the Protein Data Bank (PDB) (www.rcsb.org).[25] The enzyme was taken, hydrogens were added, and undesired agents such as water and ions were removed from the target protein. Their positions of COX-2 were subsequently optimized using CHARMm force field and the adopted-basis Newton–Raphson (ABNR) method[17] available in the DS 3.5 protocol until the root mean square deviation (RMSD) gradient was

< 0.05 kcal/mol Å^2. The binding site was defined from protein cavities. The binding sphere for 1CX2 (27, 7.23, 18.29, 22) was selected from the active site using the binding site tools.

In the molecular docking process, COX-2 enzyme was held rigid while the ligands were allowed to be flexible during refinement. CDOCKER, which includes conformer generation, docking, and scoring, was performed using the default settings. After this step, the Analyze Ligand Poses subprotocol in DS 3.5 was applied to calculate the interactions containing hydrogen bonds and bumps between ligand atoms and the enzyme. Finally, binding energies were also calculated by applying the Calculate Binding Energy subprotocol in DS 3.5 using the in situ ligand minimization step in the ABNR method. The best score, which included the largest minus CDOCKER energy and the lowest minus CDOCKER interaction energy (RMSD must be less than 2) of each ligand–enzyme complex was selected. Additionally, the lowest binding energy was taken as the best-docked conformation of the investigated compounds for the macromolecule in the molecular docking study.

Acknowledgments

This study was supported by a grant from Hacettepe University Research Center (Project no: 013D07601004). Sincere thanks to Prof Dr Esin Akı and her research group for technical support.

References

1. Vane, J. R. *Nature-New Biol.* **1971**, *231*, 232–235.
2. Unsal-Tan, O.; Ozden, K.; Rauk, A.; Balkan, A. *Eur J. Med. Chem.* **2010**, *45*, 2345–2352.
3. Pratico, D.; Dogne, J. M. *Circulation* **2005**, *112*, 1073–1079.
4. Watson, D. J.; Rhodes, T.; Cai, B.; Guess, H. A. *Arch. Intern. Med.* **2002**, *162*, 1105–1110.
5. Farkouh, M. E.; Greenberg, J. D.; Jeger, R. V.; Ramanathan, K.; Verheugt, F. W. A.; Chesebro, J. H.; Kirshner, H.; Hochman, J. S.; Lay, C. L.; Ruland, S.; et al. *Ann. Rheum. Dis.* **2007**, *66*, 764–770.
6. Biskupiak, J. E.; Brixner, D. I.; Howard, K.; Oderda, G. M. *J. Pain Pall. Care Pharmacother.* **2006**, *20*, 7–14.
7. Chan, F. K. *Nat. Clin. Pract. Gastroenterol. Hepatol.* **2006**, *3*, 563–573.
8. Garcia Rodriguez, L. A.; Jick, H. *Lancet* **1994**, *343*, 769–772.
9. Leach, A. *Molecular Modelling: Principles and Applications*; Prentice Hall: Upper Saddle River, NJ, USA, 2001.
10. Friedman, R. *Biochem. J.* **2011**, *438*, 415–426.
11. Uzgoren-Baran, A.; Tel, B. C.; Sarigol, D.; Ozturk, E. I., Kazkayasi, I.; Okay, G.; Ertan, M.; Tozkoparan, B. *Eur J. Med. Chem.* **2012**, *57*, 398–406.
12. Nakka, M.; Begum, M. S.; Varaprasad, B. F. M.; Reddy, L. V.; Bhattacharya, A.; Helliwell, M.; Mukherjee, A. K.; Beevi, S. S.; Mangamoori, L. N.; Mukkanti, K.; et al. *J. Chem. Pharm. Res.* **2010**, *2*, 393–409.
13. Palla, G.; Predieri, G.; Domiano, P.; Vignali, C.; Turner, W. *Tetrahedron* **1986**, *42*, 3649–3654.
14. Podyachev, S. N.; Litvinov, I. A.; Shagidullin, R. R.; Buzykin, B. I.; Bauer, I.; Osyanina, D. V.; Awakumova, L. V.; Sudakova, S. N.; Habicher, W. D.; Konovalov, A. I.; et al. *Spectrochim. Acta A* **2007**, *66*, 250–261.
15. Gaussian 09, Revision A.1, Frisch, M. J.; Trucks, G. W.; Schlegel, H. B.; Scuseria, G. E.; Robb, M. A.; Cheeseman, J. R.; Scalmani, G.; Barone, V.; Mennucci, B.; Petersson, G. A.; et al. Gaussian, Inc., Wallingford, CT, USA, 2009.
16. Accelrys Software Inc., Discovery Studio 3.5, San Diego, CA, USA, 2013.
17. Brooks, B. R.; Bruccoleri, R. E.; Olafson, B. D.; States, D. J.; Swaminathan, S.; Karplus, M. *J. Comput. Chem.* **1983**, *4*, 187–217.
18. Parr, R. G.; Szentpaly, L. V.; Liu, S. *J. Am. Chem. Soc.* **1999**, *121*, 1922.
19. Maynard, A. T.; Huang, M.; Rice, W. G.; Covell, D. G. *Proc. Natl. Acad. Sci. USA* 95, **1998**, 11578–11583.
20. Chattaraj, P. K.; Giri, S.; Duley, S. *Chem. Rev.* **2011**, *111*, 43–75.
21. Taskin T.; Sevin, F. *J. Mol. Struct* **2007**, *803*, 61–66.
22. Karelson, M.; Lobanov, V. S.; Katritzky, A. R. *Chem. Rev.* **1996**, *96*, 1027–1043.
23. Parthasarathi, R.; Subramanian, V.; Royb, D. R.; and Chattaraj, P. K. *Bioorg. Med. Chem.* **2004**, *12*, 5533–5543.
24. Taşkın, T., Sevin, F. *Turk. J. Chem.* **2011**, *35*, 481–498.
25. Kurumbail, R. G.; Stevens, A.M.; Gierse, J. K.; McDonald, J. J.; Stegeman, R. A.; Pak, J. Y.; Gildehaus, D.; Miyashiro, J. M.; Penning, T. D.; Seibert, K.; et al. *Nature* **1996**, *384*, 644–648.